Numerical studies of Galerkin-type time-discretizations applied to transient convection-diffusion-reaction equations

Naveed Ahmed and Gunar Matthies

Abstract—We deal with the numerical solution of time-dependent convection-diffusion-reaction equations. We combine the local projection stabilization method for the space discretization with two different time discretization schemes: the continuous Galerkin-Petrov (cGP) method and the discontinuous Galerkin (dG) method of polynomial of degree k. We establish the optimal error estimates and present numerical results which shows that the cGP(k) and dG(k)-methods are accurate of order $k + 1$, respectively, in the whole time interval. Moreover, the cGP(k)-method is superconvergent of order $2k$ and dG(k)-method is of order $2k + 1$ at the discrete time points. Furthermore, the dependence of the results on the choice of the stabilization parameter are discussed and compared.

Keywords—convection-diffusion-reaction equations, stabilized finite elements, discontinuous Galerkin, continuous Galerkin-Petrov

I. Introduction

Numerical simulations of time-dependent convection-diffusion-reaction equations requires numerical schemes of high order of accuracy both in space and in time. We consider the vertical method of lines where the spatial discretization by finite element methods is applied first. A large system of ordinary differential equations appear which is then solved numerically by a suitable time discretization. If we look, for instance, to A-stable BDF-methods, then their order is restricted to two. If we want to have an A-stable higher order time discretization, we arrive at Runge-Kutta methods or at Galerkin-type methods with higher polynomial order [11].

In this paper, we will consider two time classes of discretizations of variational type to solve time-dependent problems. The first one is the discontinuous Galerkin (dG) time stepping scheme in which both trial and test functions are discontinuous in time [25]. In the second scheme, the trial functions are continuous in time whereas the test functions are discontinuous in time. This method can be viewed as a Petrov-Galerkin method. The continuous Galerkin-Petrov (cGP) method has been studied in [3] for heat equation. A numerical comparison of cGP and dG methods applied to the heat equation is given in [14]. Recently, in [24], [21], the cGP method has been investigate for linear and nonlinear ordinary differential equations. The cGP methods are A-stable whereas it is well-known that the dG methods are even strongly A-stable (or L-stable

according to [11]), i.e., the dG methods have better damping properties with respect to high frequency error components.

In applications, the size of the diffusion is often much smaller than the size of the convection. Hence, the solutions contain layers. The use of standard Galerkin methods in space results in oscillations in the numerical solution even outside the layers. A number of finite element methods has been developed to avoid this non-physical effect, for example residual based methods like the streamline upwind Petrov-Galerkin (SUPG) method [13] or Galerkin least squares FEM [23]. However, the combination of the SUPG method with higher order schemes in time is not straightforward. Indeed, the discrete time derivative, the source term and second order derivatives have to be included into the stabilization term to ensure the consistency of the method. An alternative to SUPG is the use of symmetric stabilization techniques such as local projection stabilization (LPS) [22], the continuous interior penalty (CIP) [5], the orthogonal subscales method (OSS) [9], [8]. A drawback of CIP, OSS and the two-level LPS methods is an increased discretization stencil due to the additional couplings between degrees of freedoms which do not belong to the same cell. It was shown in [12] that the two-level variant of the LPS can be also considered as an enriched one-level method on the coarser mesh. This enables to reduce the degrees of freedom in the two-level method without losing the convergence rate.

Stabilized finite element methods for time-dependent convection-diffusion-reaction problems have been investigated by several authors. We refer to [20], [7] which consider different stabilization techniques including SUPG and to [9] using OSS. SUPG methods in space combined with the backward Euler and the Crank-Nicolson method in time are studied in [16]. The CIP in space combined with the θ-method in time has been investigated in [4]. The coupling of other stabilization techniques in the one dimensional case with the finite difference time integration, in particular, vertical and horizontal methods of lines have been discussed in [2]. The dG method has been analyzed in time combined with LPS in space in [1] and in space and time [10].

In this paper, we consider the the one-level local projection method for the space discretization in combination with two different higher order time discretization schemes: the continuous Galerkin-Petrov (cGP) and discontinuous Galerkin (dG) methods.

We consider the problem:

Naveed Ahmed, Universität Kassel, Fachbereich 10 Mathematik und Naturwissenschaften, Institut für Mathematik, Heinrich-Plett-Straße 40, 34132 Kassel, Germany, e-mail: nahmed@mathematik.uni-kassel.de

Gunar Matthies, Universität Kassel, Fachbereich 10 Mathematik und Naturwissenschaften, Institut für Mathematik, Heinrich-Plett-Straße 40, 34132 Kassel, Germany e-mail: matthies@mathematik.uni-kassel.de

Find $u : \Omega \times (0,T) \to \mathbb{R}$ such that

$$\begin{cases} u' - \varepsilon\Delta u + \mathbf{b}\cdot\nabla u + \sigma u = f & \text{in } \Omega \times (0,T), \\ u = 0 & \text{on } \partial\Omega \times (0,T), \\ u(\cdot,0) = u_0 & \text{in } \Omega, \end{cases} \quad (1)$$

where Ω is a polygonal domain in $\mathbb{R}^d$, $d = 1$, 2, or 3, with a polyhedral boundary $\partial\Omega$, T the final time, $\varepsilon > 0$ the diffusion coefficient, $\mathbf{b} \in W^{1,\infty}(\Omega)$ the convection field, $\sigma \in L^\infty(\Omega)$ the reaction coefficient, $u_0(x)$ the given initial data and f describes sources. We assume that the data $\mathbf{b}$, σ, u_0 and f are sufficiently smooth on Ω and $\Omega \times (0,T)$, respectively.

In the following, it is assumed that there is a constant $\sigma_0 > 0$ such that

$$\sigma - \frac{1}{2}\nabla\cdot\mathbf{b} \geq \sigma_0 > 0 \qquad \text{in } \Omega.$$

This is a standard assumption in the analysis of equations of type (1), see [23].

Throughout this paper, standard notations and conventions will be used. Let $H^m(\Omega)$ denote the Sobolev space of functions with derivatives up to order m in $L^2(\Omega)$. We denote by $(\cdot,\cdot)$ the inner product in $L^2(\Omega)$ and by $\|\cdot\|_0$ the associated L^2-norm. The norm in $H^m(\Omega)$ is defined as

$$\|v\|_m = \left(\sum_{|\alpha|\leq m} \|D^\alpha v\|_0^2 \right)^{1/2}.$$

We consider also certain Bochner spaces. To this end, let X be a Banach space equipped with the norm $\|\cdot\|_X$. Then, we define

$$C(0,T;X) = \left\{ v : [0,T] \to X, \quad v \text{ continuous} \right\},$$

$$L^2(0,T;X) = \left\{ v : (0,T) \to X, \quad \int_0^T \|v(t)\|_X^2 dt < \infty \right\},$$

$$H^m(0,T;X) = \left\{ v \in L^2(0,T;X) : \frac{\partial^j v}{\partial t^j} \in L^2(0,T;X), \right.$$
$$\left. 1 \leq j \leq m \right\},$$

where the derivatives $\partial^j v/\partial t^j$ are understood in the sense of distributions on $(0,T)$. In the following we use the short notation $Y(X) := Y(0,T;X)$. The norms and seminorms in the above defined spaces are given by

$$\|v\|_{C(X)} = \sup_{t\in[0,T]} \|v(t)\|_X, \qquad \|v\|_{L^2(X)}^2 = \int_0^T \|v(t)\|_X^2 dt,$$

$$\|v\|_{H^m(X)}^2 = \int_0^T \sum_{j=0}^m \left\| \frac{\partial^j v}{\partial t^j} \right\|_X^2 dt.$$

II. SPACE DISCRETIZATION

In order to introduce a variational setting for (1) we consider the space $V = H_0^1(\Omega)$ consisting of functions vanishing on the boundary. Finite element methods employ now a finite dimensional space $V_h \subset V$ of continuous elements of order

$r \geq 1$, where h indicates the fineness of the underlying triangulation $\mathcal{T}_h$. With the usual bilinear form

$$a(u,v) := (\varepsilon\nabla u, \nabla v) + (\mathbf{b}\cdot\nabla u + \sigma u, v) \qquad (2)$$

associated with the problem (1), a Galerkin formulation arising from (1) reads as follows:

Find $u_h : [0,T] \to V_h$ such that $u_h(0) = u_{h,0}$ and

$$(u_h', v_h) + a(u_h, v_h) = (f, v_h) \quad \forall v_h \in V_h \qquad (3)$$

with $u_{h,0} \in V_h$ as a suitable approximation of u_0.

It is well known that in the convection-dominated case standard finite element methods will lead to discrete solutions which contain global unphysical oscillations. In order to prevent this, we will consider the one-level LPS to stabilize the space discretization in which approximation and projection spaces live on the same mesh. Let $\mathcal{D}_h(K)$, $K \in \mathcal{T}_h$, be finite dimensional spaces and $\pi_K : L^2(K) \to \mathcal{D}_h(K)$ the local L^2 projection into $D_h(K)$. The projection space D_h is given by

$$D_h := \bigoplus_{K\in\mathcal{T}_h} D_h(K).$$

We define the global projection operator $\pi_h : L^2(\Omega) \to D_h$ by $(\pi_h v)|_K := \pi_K(v|_K)$. The fluctuation operator $\kappa_h : L^2(\Omega) \to L^2(\Omega)$ is given by $\kappa_h := id - \pi_h$, where $id : L^2(\Omega) \to L^2(\Omega)$ is the identity mapping in $L^2(\Omega)$. The stabilization term S_h is defined by

$$S_h(u_h, v_h) := \sum_{K\in\mathcal{T}_h} \mu_K \big(\kappa_h\nabla u_h, \kappa_h\nabla v_h\big)_K \qquad (4)$$

Here, $K \in \mathcal{T}_h$ denotes the mesh cells of the triangulation, $(\cdot,\cdot)_K$ the inner product in $L^2(K)$, and μ_K the user chosen non-negative constant. The stabilization term gives additional control over the fluctuation of gradients. Note that one can replace the gradient ∇w_h by the derivative in streamline direction $\mathbf{b}\cdot\nabla w_h$ or (even better [18], [19]) by $\mathbf{b}_K\cdot\nabla w_h$ where $\mathbf{b}_K$ is a piecewise constant approximation of $\mathbf{b}$, which leads to similar results.

Now the stabilized semi-discrete problem reads:
Find $u_h : [0,T] \to V_h$ such that $u_h(0) = u_{h,0}$ and

$$(u_h', v_h) + a_h(u_h, v_h) = (f, v_h) \qquad \forall v_h \in V_h \qquad (5)$$

where

$$a_h(u,v) := a(u,v) + S_h(u,v). \qquad (6)$$

Let us introduce the mesh-dependent norm on the space V_h by

$$|||v||| := \left(\varepsilon|v|_1^2 + \sigma_0\|v\|_0^2 + \sum_{K\in\mathcal{T}_h} \mu_k\|\kappa_h\nabla v\|_{0,K}^2 \right)^{1/2}.$$

Stability and convergence properties of the LPS method (5) are based on the following assumptions with respect to the pair (V_h, D_h), see [22], [23].

Assumption A1: There is an interpolation operator $j_h : H^2(\Omega) \to V_h$ such that for all $K \in \mathcal{T}_h$, $v \in H^l(K)$, and $2 \leq l \leq r+1$, the interpolation error estimate

$$\|v - j_h v\|_{0,K} + h_K|v - j_h v|_{1,K} \leq Ch_k^l\|v\|_{l,K}$$

and the orthogonality

$$(v - j_h v, q_h) = 0 \qquad \forall q_h \in \mathcal{D}_h, \forall v \in H^2(\Omega)$$

hold true.

Assumption A2: The fluctuation operator κ_h satisfies the following approximation property

$$\|\kappa_h q\|_{0,K} \leq C h_K^l |q|_{l,K} \quad \forall K \in \mathcal{T}_h, \ \forall q \in H^l(K), \ 0 \leq l \leq r.$$

For the stationary problem associated with (1) we have

Theorem 1. *Suppose A1 and A2, $\mu_K \sim h_K$ for all $K \in \mathcal{T}_h$ and let the data of the problem be sufficiently smooth. Then there exists a positive constant C independent of ε and h, such that*

$$|||w - j_h w||| \leq C(\varepsilon^{1/2} + h^{1/2}) h^r \|w\|_{r+1}$$

for all $w \in H^{r+1}(\Omega) \cap H_0^1(\Omega)$.

For more detail, see [23], [22].

III. TIME DISCRETIZATION

We discretize the problem (5) in time using the continuous Galerkin-Petrov method (cGP) and the discontinuous Galerkin method (dG). To this end, we decompose the time interval $J = (0, T]$ into N sub-intervals $J_n := (t_{n-1}, t_n]$ of length $\tau_n = t_n - t_{n-1}$, where $n = 1, \ldots, N$, $0 = t_0 < t_1 < \cdots < t_{N-1} < t_N = T$, $\tau = \max_{1 \leq n \leq N} \tau_n$. In the following, the set of the time intervals $\mathcal{M}_\tau$ will be called the time-mesh. For any positive integer k, the discontinuous and continuous spaces are defined as

$$Y_k := \{v \in L^2(J, V_h) : v|_{J_n} \in \mathbb{P}_k(J_n, V_h) \quad \forall J_n \in \mathcal{M}_\tau\},$$
$$X_k := \{u \in C(J, V_h) : u|_{J_n} \in \mathbb{P}_k(J_n, V_h) \quad \forall J_n \in \mathcal{M}_\tau\},$$

where

$$\mathbb{P}_k(J_n, V) := \left\{ u : J_n \to V : u(t) \sum_{j=0}^{k} U^j t^j \right\}$$

is the space of V_h-valued polynomials in time of order k.

A. The cGP(k) method

In this method, we use the space X_k as the fully discrete solution space and Y_k as the discrete test space. The fully discrete cGP(k) method is defined as follows:
Find $U \in X_k$ such that $U(0) = u_{h,0}$ and

$$\int_0^T \left\{ (U', \psi) + a_h(U, \psi) \right\} = \int_0^T (f, \psi) \tag{7}$$

for all $\psi \in Y_k$. Since the discrete test space is discontinuous in time, problem (7) can be solved by a time-marching process where successively local problems on the time intervals J_n are solved. We consider the mesh-dependent norm

$$\|v\|_{cGP} := \left(\int_0^T \left\{ \|v'\|_0^2 + |||v|||^2 \right\} \right)^{1/2}.$$

The following result states an a priori error estimate for the fully discrete formulation (7), which is derived using the idea from [21], [24].

Theorem 2. *Suppose A1, A2, and $\mu_K \sim h_K$ for all $K \in \mathcal{T}_h$. Let U and u be the solutions of the fully discrete problem (7) and the continuous problem (1). Moreover, let $u \in H^1(H^{r+1})$. Then there exists a positive constant C independent of h, τ and ε, such that the error estimate*

$$\|U - u\|_{cGP} \leq C\left(\tau^k + (\varepsilon^{1/2} + h^{1/2}) h^r \right) \tag{8}$$

holds true.

B. The dG(k) method

Here the discrete solution space is the same as the test space, namely Y_k. The fully discrete dG(k) method reads:
Find $U \in Y_k$ such that

$$\sum_{n=1}^{N} \int_{J_n} \left\{ (U', \psi) + a_h(U, \psi) \right\} + \sum_{n=1}^{n-1} ([U]_n, \psi) + (U_0^+, \psi_0^+)$$
$$= (u_0, \psi_0^+) + \int_0^T (f, \psi) \tag{9}$$

for all $\psi \in Y_k$, where the left-sided value u_0^-, right-sided value u_n^+ and the jump $[u]_n$ are defined as

$$u_n^- := \lim_{t \to t_n - 0} u(t), \ u_n^+ := \lim_{t \to t_n + 0} u(t), \ [u]_n := u_n^+ - u_n^-.$$

Due to the discontinuity in time of the discrete test space, a time-marching process can be used to solve (9). We consider the following mesh-dependent norm for the dG time discretization method

$$\|v\|_{dG} := \left(\sum_{n=1}^{N} |||v|||^2 + \frac{1}{2} \|v_0^+\|_0^2 \right.$$
$$\left. + \frac{1}{2} \sum_{n=1}^{N-1} \|[v]_n\|_0^2 + \frac{1}{2} \|v_N^-\|_0^2 \right)^{1/2}.$$

The next theorem states the main results from [1].

Theorem 3. *Suppose A1, A2, and $\mu_K \sim h_K$ for all $K \in \mathcal{T}_h$. Let U and u be the solutions of the fully discrete problem (9) and the continuous problem (1), respectively. Moreover, let $u \in H^1(H^{r+1})$. Then there exists a positive constant C independent of h, τ and ε, such that the error estimate*

$$\|U_h - u\|_{dG} \leq C\left(\tau^{k+1/2} + (\varepsilon^{1/2} + h^{1/2}) h^r \right)$$

holds true.

IV. NUMERICAL STUDIES

This section will present some numerical results for the cGP and dG methods in time combined with LPS method in space. All numerical calculation were performed with the finite element package MooNMD [15].

In our numerical computations, we use the mapped finite element spaces [6] where the enriched spaces on the reference cell $\widehat{K}$ are given by

$$P_r^{\text{bubble}}(\widehat{K}) := P_r(\widehat{K}) + \hat{b}_\triangle P_{r-1}(\widehat{K}),$$
$$Q_r^{\text{bubble}}(\widehat{K}) := Q_r(\widehat{K}) + \text{span}\{\hat{b}_\square \hat{x}_i^{r-1}, \ i = 1, 2\}.$$

Here, $\hat{b}_\triangle$ and $\hat{b}_\square$ are the cubic bubble on the reference triangle and the biquadratic bubble on the reference square, respectively. The pairs $(P_r^{\text{bubble}}, P_{r-1}^{\text{disc}})$, $r \geq 1$, on triangles and the pairs $(Q_r^{\text{bubble}}, P_{r-1}^{\text{disc}})$, $r \geq 1$, on quadrilaterals fulfill the assumptions A1 and A2. Further examples of spaces (V_h, D_h) satisfying A1 and A2 are given in [22], [23].

The numerical tests have used for $(V_h, \mathcal{D}_h)$ the pairs $(Q_r^{\text{bubble}}, P_{r-1}^{disc})$ and $(P_r^{\text{bubble}}, P_{r-1}^{disc})$, $r = 1, 2, 3$. The stabilization parameters μ_K have been chosen as

$$\mu_K = \mu_0 h_K \qquad \forall K \in \mathcal{T}_h$$

where μ_0 denotes a constant which will be given for each of the test calculations.

Example 1. We consider as example a pure transport problem in two dimensions: a rotating Gaussian benchmark taken from [4]. Hence, we consider (1) in

$$\Omega = \{(x, y) \in \mathbb{R}^2 : \ x^2 + y^2 \leq 1\}$$

with the data

$$\varepsilon = 0, \ b = (-y, x)^T, \ \sigma = f = 0,$$

and the Gaussian initial condition

$$u_0(x, y) = \exp\left(-10(x - 0.3)^2 - 10(y - 0.3)^2)\right)$$

is centered at $(0.3, 0.3)$. In order to illustrate the convergence order in time of the discrete solution, we have chosen a finite element space based on P_3^{bubble} with projection onto P_2^{disc} on a relatively fine mesh consisting of $32,768$ cells. The coefficient in the stabilization parameter is set to $\mu_0 = 0.1$. We evaluate the results of our calculations by considering the following norms

$$\|e\|_{L^2(J, V_h)} := \left(\int_0^T \|e\|_{V_h}^2 \, dt\right)^{1/2},$$

$$\|e\|_{l_\infty(J, V_h)} := \max_{1 \leq n \leq N} \|e(t_n)\|_{V_h}.$$

In Tables I-III, we report the convergence orders at $T = 2\pi$ (one complete rotation) of the discrete solution obtained with the cGP(k)-method with $k \in \{1, 2, 3\}$. The predicted orders for the error and its time derivative in the integral-based norm $\|\cdot\|_{L^2(J, V_h)}$ are confirmed.

For heat equation, it was shown in [3] that the cGP(k) method are superconvergent of order $2k$ in the discrete time points t_n. We can observe the order $2k$ for cGP(k) method with $k \in \{1, 2, 3\}$ also for the time-dependent convection-diffusion equation with the local projection method as spatial stabilization.

Furthermore, we also present norms of the error $\tilde{e} = u - \tilde{U}$. $\tilde{U}$ represents the post-processed solution $\tilde{U}$ which is obtained by means of a simple post-processing from the solution U of the original cGP(k)-method. It was shown in [21] that for $k \geq$

2 at least a superconvergence of order $k+2$ can be obtained for the cGP(k)-method. From the results of Tables IV-VI, we see that expected convergence orders are achieved for cGP(1) and cGP(2). For cGP(3), the error start decreasing for smaller time step length. This is because of the error in space dominates, i.e., the mesh size is not small enough to see the corresponding convergence order in time.

TABLE I
ERRORS AND CONVERGENCE ORDERS FOR CGP(1), WHERE $e = u - U$.

τ	$\|e\|_{L^2(J,V_h)}$		$\|d_t e\|_{L^2(J,V_h)}$		$\|e\|_{l_\infty(J,V_h)}$		$\|e\|_{\text{cGP}}$	
	error	order	error	order	error	order	error	order
$2\pi/10$	2.768-1		6.695-1		1.778-1		7.244-1	
$2\pi/20$	1.136-1	1.29	3.574-1	0.91	7.673-2	1.21	3.750-1	0.95
$2\pi/40$	3.434-2	1.73	1.373-1	1.38	2.364-2	1.70	1.415-1	1.41
$2\pi/80$	9.005-3	1.93	5.087-2	1.43	6.196-3	1.93	5.166-2	1.45
$2\pi/160$	2.276-3	1.99	2.193-2	1.21	1.564-3	1.99	2.205-2	1.23
$2\pi/320$	5.704-4	2.00	1.046-2	1.07	3.917-4	2.00	1.047-2	1.07
theoret. order:	2		1		2		1	

TABLE II
ERRORS AND CONVERGENCE ORDERS FOR CGP(2), WHERE $e = u - U$.

τ	$\|e\|_{L^2(J,V_h)}$		$\|d_t e\|_{L^2(J,V_h)}$		$\|e\|_{l_\infty(J,V_h)}$		$\|e\|_{\text{cGP}}$	
	error	order	error	order	error	order	error	order
$2\pi/10$	3.031-2		1.312-1		2.036-2		1.347-1	
$2\pi/20$	2.981-3	3.35	2.181-2	2.59	1.967-3	3.37	2.201-2	2.61
$2\pi/40$	2.257-4	3.72	4.559-3	2.26	1.359-4	3.86	4.565-3	2.27
$2\pi/80$	1.856-5	3.60	1.120-3	2.03	8.703-6	3.97	1.120-3	2.03
$2\pi/160$	1.873-6	3.31	2.797-4	2.00	5.472-7	3.99	2.797-4	2.00
theoret. order:	3		2		4		2	

TABLE III
ERRORS AND CONVERGENCE ORDERS FOR CGP(3), WHERE $e = u - U$.

τ	$\|e\|_{L^2(J,V_h)}$		$\|d_t e\|_{L^2(J,V_h)}$		$\|e\|_{l_\infty(J,V_h)}$		$\|e\|_{\text{cGP}}$	
	error	order	error	order	error	order	error	order
$2\pi/10$	2.284-3		1.633-2		1.460-3		1.649-2	
$2\pi/20$	7.299-5	4.97	1.610-3	3.34	3.377-5	5.43	1.612-3	3.36
$2\pi/40$	3.443-6	4.41	2.002-4	3.01	5.815-7	5.86	2.002-4	3.01
$2\pi/80$	2.095-7	4.04	2.508-5	3.00	1.347-8	5.43	2.508-5	3.00
theoret. order:	4		3		6		3	

TABLE IV
ERRORS AND CONVERGENCE ORDERS FOR CGP(1), WHERE $\tilde{e} = u - \tilde{U}$.

τ	$\|\tilde{e}\|_{L^2(J,V_h)}$		$\|d_t \tilde{e}\|_{L^2(J,V_h)}$		$\|d_t \tilde{e}\|_{l_\infty(J,V_h)}$	
	error	order	error	order	error	order
$2\pi/10$	2.946-1		6.661-1		3.990-1	
$2\pi/20$	1.164-1	1.34	3.336-1	1.00	2.190-1	0.87
$2\pi/40$	3.448-2	1.76	1.119-1	1.58	7.683-2	1.51
$2\pi/80$	8.974-3	1.94	3.015-2	1.90	2.080-2	1.89
$2\pi/160$	2.263-3	1.99	7.660-3	1.98	5.277-3	1.98
$2\pi/320$	5.669-4	2.00	1.922-3	2.00	1.323-3	2.00
theoret. order:	2		2		2	

TABLE V
ERRORS AND CONVERGENCE ORDERS FOR CGP(2), WHERE $\tilde{e} = u - \tilde{U}$.

τ	$\|\tilde{e}\|_{L^2(J,V_h)}$		$\|d_t \tilde{e}\|_{L^2(J,V_h)}$		$\|d_t \tilde{e}\|_{l_\infty(J,V_h)}$	
	error	order	error	order	error	order
$2\pi/10$	3.008-2		1.165-1		7.787-2	
$2\pi/20$	2.853-3	3.40	1.302-2	3.16	8.765-3	3.15
$2\pi/40$	1.974-4	3.85	9.799-4	3.73	6.253-4	3.81
$2\pi/80$	1.264-5	3.97	7.519-5	3.70	4.034-5	3.95
$2\pi/160$	7.955-7	3.99	8.749-6	3.10	2.694-6	3.91
theoret. order:	4		3		4	

In Tables VII-IX, we report the errors and convergence orders obtained for the discontinuous Galerkin method dG(k) with $k \in \{1, 2, 3\}$. Optimal convergence with respect to the integral-based norm was again obtained, see Theorem 3. It

TABLE VI
ERRORS AND CONVERGENCE ORDERS FOR CGP(3), WHERE $\tilde{e} = u - \tilde{U}$.

τ	$\|\tilde{e}\|_{L^2(J,V_h)}$		$\|d_t\tilde{e}\|_{L^2(J,V_h)}$		$\|d_t\tilde{e}\|_{l_\infty(J,V_h)}$	
	error	order	error	order	error	order
$2\pi/10$	2.137-3		1.143-2		7.531-3	
$2\pi/20$	5.011-5	5.41	3.533-4	5.02	1.915-4	5.30
$2\pi/40$	9.272-7	5.76	1.910-5	4.21	6.735-6	4.83
$2\pi/80$	6.064-8	3.94	6.609-6	1.53	8.941-7	2.91
theoret. order:		5		4		6

TABLE XI
ERRORS AND CONVERGENCE ORDERS FOR dG(2), WHERE $\tilde{e} = u - \tilde{U}$.

τ	$\|\tilde{e}\|_{L^2(J,V_h)}$		$\|d_t\tilde{e}\|_{L^2(J,V_h)}$		$\|d_t\tilde{e}\|_{l_\infty(J,V_h)}$	
	error	order	error	order	error	order
$2\pi/10$	8.017-3		3.802-2		2.179-2	
$2\pi/20$	4.273-4	4.23	3.215-3	3.56	1.405-3	3.96
$2\pi/40$	1.592-5	4.75	3.196-4	3.33	5.144-5	4.77
$2\pi/80$	6.221-7	4.68	3.895-5	3.04	1.917-6	4.75
$2\pi/160$	3.663-8	4.09	4.862-6	3.00	8.930-7	1.10
theoret. order:		4		3		5

TABLE XII
ERRORS AND CONVERGENCE ORDERS FOR dG(3), WHERE $\tilde{e} = u - \tilde{U}$.

τ	$\|\tilde{e}\|_{L^2(J,V_h)}$		$\|d_t\tilde{e}\|_{L^2(J,V_h)}$		$\|d_t\tilde{e}\|_{l_\infty(J,V_h)}$	
	error	order	error	order	error	order
$2\pi/10$	5.611-4		4.13-3		1.979-3	
$2\pi/20$	8.709-6	6.01	1.949-4	4.41	2.722-5	6.18
$2\pi/40$	1.913-7	5.51	1.206-5	4.02	9.271-7	4.88
theoret. order:		5		4		7

was proved in [25] that the dG(k) method is superconvergent of order $2k + 1$ in the discrete time points t_n for an abstract symmetric model problem like the heat equation. We can also observe the order $2k + 1$ for dGk method with $k \in \{1, 2, 3\}$.

In X-XII, errors and convergence history of post-processed solution associated with the discontinuous Galerkin method are presented. In [21], the superconvergence of order $k + 2$ for dG(k) method, $k \geq 1$, are obtained for the Burgers equations as a test problem. In our model problem, we also see that the dG(k) method is superconvergent of order $k + 2$.

TABLE VII
ERRORS AND CONVERGENCE ORDERS FOR DG(1), WHERE $e = u - U$.

τ	$\|e\|_{L^2(J,V_h)}$		$\|d_t e\|_{L^2(J,V_h)}$		$\|e\|_{l_\infty(J,V_h)}$		$\|e\|_{dG}$	
	error	order	error	order	error	order	error	order
$2\pi/10$	8.792-2		3.873-1		4.986-2		1.177-1	
$2\pi/20$	2.170-2	2.02	1.936-1	1.00	1.253-2	1.99	4.093-2	1.52
$2\pi/40$	4.052-3	2.42	9.503-2	1.03	2.051-3	2.61	1.379-2	1.57
$2\pi/80$	7.884-4	2.36	4.745-2	1.00	2.734-4	2.91	4.779-3	1.53
$2\pi/160$	1.775-4	2.15	2.373-2	1.00	3.458-5	2.98	1.676-3	1.51
$2\pi/320$	4.301-5	2.01	1.187-2	1.00	4.332-6	3.00	5.903-4	1.51
theoret. order:		2		1		3		1.5

TABLE VIII
ERRORS AND CONVERGENCE ORDERS FOR DG(2), WHERE $e = u - U$.

τ	$\|e\|_{L^2(J,V_h)}$		$\|d_t e\|_{L^2(J,V_h)}$		$\|e\|_{l_\infty(J,V_h)}$		$\|e\|_{dG}$	
	error	order	error	order	error	order	error	order
$2\pi/10$	9.5673		8.816-2		5.134-3		1.834-2	
$2\pi/20$	8.409-4	3.51	2.332-2	1.92	2.813-4	4.19	3.242-3	2.50
$2\pi/40$	9.311-5	3.18	5.966-3	1.97	9.909-6	4.83	5.707-4	2.51
$2\pi/80$	1.151-5	3.02	1.499-3	1.99	3.174-7	4.96	1.002-4	2.51
$2\pi/160$	1.438-6	3.00	3.751-4	2.00	1.394-8	4.51	1.76-5	2.51
theoret. order:		3		2		5		2.5

TABLE IX
ERRORS AND CONVERGENCE ORDERS FOR DG(3), WHERE $e = u - U$.

τ	$\|e\|_{L^2(J,V_h)}$		$\|d_t e\|_{L^2(J,V_h)}$		$\|e\|_{l_\infty(J,V_h)}$		$\|e\|_{dG}$	
	error	order	error	order	error	order	error	order
$2\pi/10$	9.036-4		1.750-2		3.548-4		2.644-3	
$2\pi/20$	4.800-5	4.23	2.370-3	2.89	4.383-6	6.34	2.434-4	3.44
$2\pi/40$	2.997-6	4.00	3.018-4	2.97	3.907-8	6.81	2.157-5	3.50
theoret. order:		4		3		7		3.5

TABLE X
ERRORS AND CONVERGENCE ORDERS FOR DG(1), WHERE $\tilde{e} = u - \tilde{U}$.

τ	$\|\tilde{e}\|_{L^2(J,V_h)}$		$\|d_t\tilde{e}\|_{L^2(J,V_h)}$		$\|d_t\tilde{e}\|_{l_\infty(J,V_h)}$	
	error	order	error	order	error	order
$2\pi/10$	8.250-2		2.483-1		1.393-1	
$2\pi/20$	1.923-2	2.10	7.224-2	1.78	4.329-2	1.69
$2\pi/40$	3.027-3	2.67	1.376-2	2.39	7.934-3	2.45
$2\pi/80$	3.989-4	2.92	2.421-3	2.51	1.093-3	2.86
$2\pi/160$	5.033-5	2.99	4.994-4	2.28	1.390-4	2.97
$2\pi/320$	6.302-6	3.00	1.170-4	2.09	1.746-5	2.99
theoret. order:		3		2		3

Example 2. This example is taken from [17]. The prescribed solution has the form

$$u(x,y;t) = 16\sin(\pi t)x(1-x)y(1-y)$$
$$\times \left(\frac{1}{2} + \frac{\arctan\left[2\varepsilon^{-1/2}w(x,y)\right]}{\pi} \right)$$

where

$$w(x,y) := (0.25^2 - (x-0.5)^2 - (y-0.5)^2.$$

This is a hump changing its height in the course of time. The steepness of the circular internal layer depends on the diffusion parameter ε. Analogue to [17], we present the simulation for $\varepsilon = 10^{-6}$, $\mathbf{b} = (2,3)$, $\sigma = 1$ and $T = 2$. We measure the size of the spurious oscillation by

$$\text{var}(t) := \max_{(x,y)\in\Omega} U(x,y;t) - \min_{(x,y)\in\Omega} U(x,y;t)$$

where the maximum and minimum were computed only in the vertices of the mesh cells.

The time step was chosen to be $\tau = 10^{-3}$ and computations were performed on a regular grid consisting of 128×128 squares. This leads to 33,025 degrees of freedom for Q_1^{bubble}, 98,817 for Q_2^{bubble} and 180,993 for Q_3^{bubble}. Note that, in the following figures only the nodal values at the cell vertices are shown, i.e., the additional bubble part of the solution will not be shown. We have performed the calculation with $\mu_0 \in \{0.01, 0.1, 1.0\}$.

The obtained numerical solutions for cGP(1) and the pair $(Q_1^{\text{bubble}}, P_0^{\text{disc}})$ with different values of stabilization parameter μ_0 in $\mu_K = \mu_0 h_K$ are presented in Fig. 1 and table XIII. We see that for the small value of $\mu_0 = 0.01$ the solution oscillates, and for large value of $\mu_0 = 1.0$ the tendency of smearing is observed, see Fig. 1 top and bottom, respectively. For a suitable value of $\mu_0 = 0.1$ the solution is captured very well but still we see some small overshoots and undershoots. The computed solutions for cGP(2) and the pair $(Q_2^{\text{bubble}}, P_1^{\text{disc}})$ with different values of μ_0 are given in Fig. 2 and table XIII. Here, the behavior of the numerical solution with respect to the stabilization parameter μ_0 is similar to the cGP(1) case. That is, the small value of $\mu_0 = 0.01$ causes oscillations and the large value $\mu_0 = 1.0$ causes smearing, see Fig. 2 top and bottom, respectively. For $\mu_0 = 0.1$ the solution is captured

very well with very small overshoots and undershoots, see Fig. 2 middle. Using cGP(3) and the pair $(Q_3^{\text{bubble}}, P_2^{\text{disc}})$, the situation changes. From Fig. 3 and Table XIII, we see that even for the small value of $\mu_0 = 0.01$ solution shows no oscillations. The solution is captured very well on almost the whole domain.

The obtained numerical results for dG(1) and the pair $(Q_1^{\text{bubble}}, P_0^{\text{disc}})$ with different values of stabilization parameters μ_0 in $\mu_K = \mu_0 h_K$ are presented in Fig. 4 and Table XIII, for dG(2) and $(Q_2^{\text{bubble}}, P_1^{\text{disc}})$ in Fig. 5 and for dG(3) and $(Q_3^{\text{bubble}}, P_2^{\text{disc}})$ in Fig. 6. It is to be noted that, there are no significant differences between the numerical solutions obtained by using the cGP(k) or dG(k) methods. Furthermore, the position of the hump is captured very well with higher order discretization schemes, see the figures 3 and 6.

TABLE XIII

HUMP CHANGING ITS HEIGHT, RESULTS OBTAINED WITH $(Q_r^{\text{BUBBLE}}, P_{r-1}^{\text{DISC}})$ WITH CGP(r) OR DG(r), $r = 1, 2, 3$.

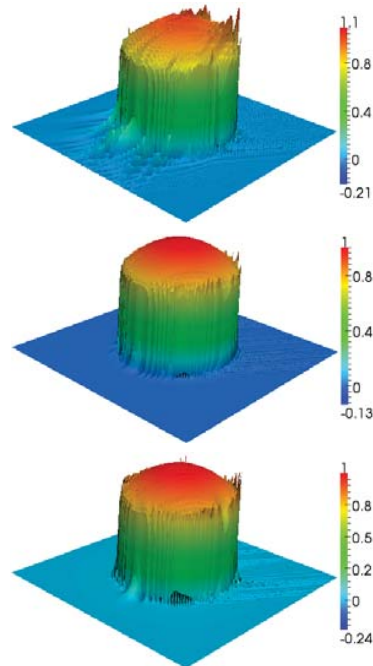| r	μ_0	var(0.5)	r	μ_0	var(0.5)
	0.01	1.174378-1		0.01	1.174996-1
1	0.1	4.381541-2	1	0.1	4.381543-2
	1.0	4.559145-2		1.0	4.559179-2
	0.01	4.047359-2		0.01	3.597300-2
2	0.1	1.860530-2	2	0.1	1.860530-2
	0.01	2.754577-2		1.0	2.754577-2
	0.01	4.339726-2		0.01	4.339726-2
3	0.1	1.700958-2	3	0.1	1.700958-2
	1.0	2.977295-2		1.0	2.977295-2

Fig. 2. Hump changing its height, the computed solution with $(Q_2^{\text{bubble}}, P_1^{\text{disc}})$ and cGP(2) at $t = 0.5$, with $\mu_0 = 0.01$, $\mu_0 = 0.1$, $\mu_0 = 1$; top to bottom.
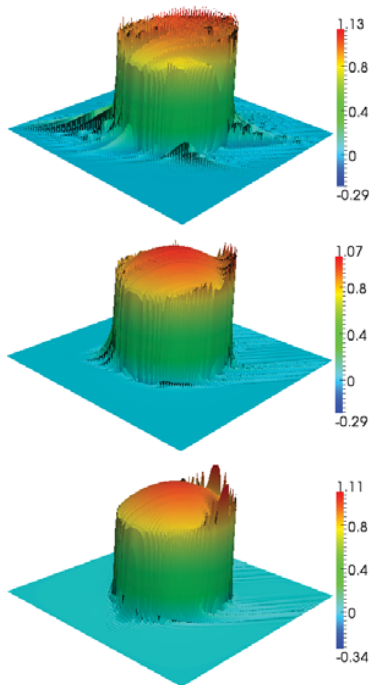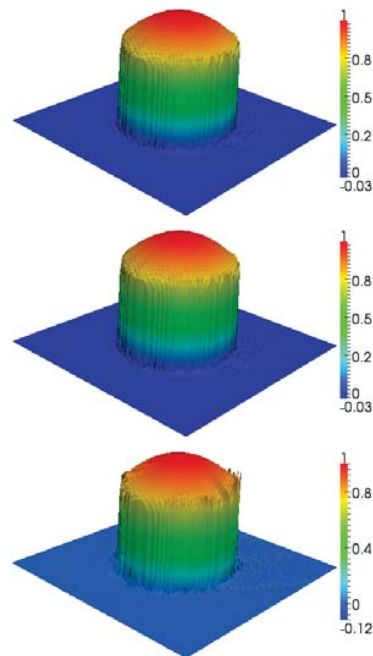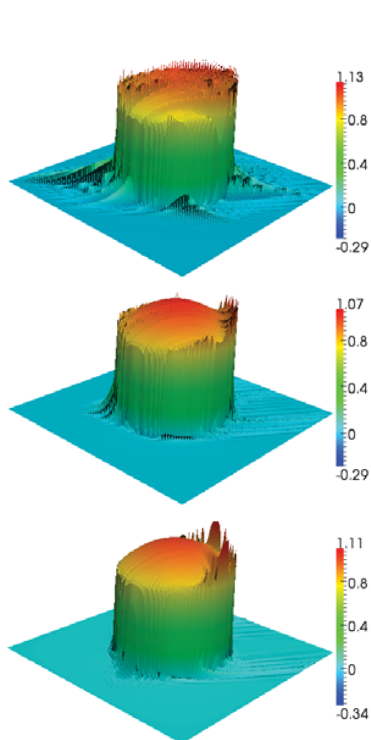

Fig. 1. Hump changing its height, the computed solution with $(Q_1^{\text{bubble}}, P_0^{\text{disc}})$ and cGP(1) at $t = 0.5$, with $\mu_0 = 0.01$, $\mu_0 = 0.1$, $\mu_0 = 1$; top to bottom.
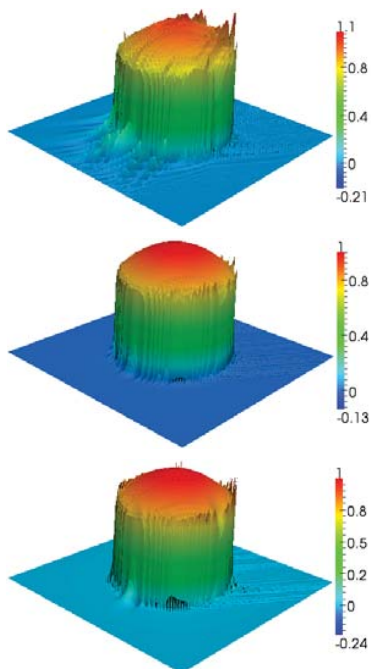

Fig. 3. Hump changing its height, the computed solution with $(Q_3^{\text{bubble}}, P_2^{\text{disc}})$ and cGP(3) at $t = 0.5$, with $\mu_0 = 0.01$, $\mu_0 = 0.1$, $\mu_0 = 1$; top to bottom.

Fig. 4. Hump changing its height, the computed solution with $(Q_1^{\text{bubble}}, P_0^{\text{disc}})$ and dG(1) at $t = 0.5$, with $\mu_0 = 0.01$, $\mu_0 = 0.1$, $\mu_0 = 1$; top to bottom.

Fig. 5. Hump changing its height, the computed solution with $(Q_2^{\text{bubble}}, P_1^{\text{disc}})$ and dG(2) at $t = 0.5$, with $\mu_0 = 0.01$, $\mu_0 = 0.1$, $\mu_0 = 1$; top to bottom.
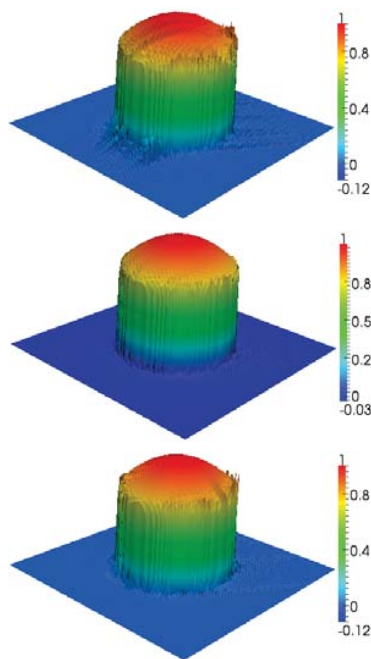

Fig. 6. Hump changing its height, the computed solution with $(Q_3^{\text{bubble}}, P_2^{\text{disc}})$ and dG(3) at $t = 0.5$, with $\mu_0 = 0.01$, $\mu_0 = 0.1$, $\mu_0 = 1$; top to bottom.

REFERENCES

[1] N. Ahmed, G. Matthies, L. Tobiska, and H. Xie. Discontinuous Galerkin time stepping with local projection stabilization for transient convection-diffusion-reaction problems. *Comput. Methods Appl. Mech. Engrg.*, 200(21-22):1747–1756, 2011.

[2] M. I. Asensio, B. Ayuso, and G. Sangalli. Coupling stabilized finite element methods with finite difference time integration for advection-diffusion-reaction problems. *Comput. Methods Appl. Mech. Engrg.*, 196(35-36):3475–3491, 2007.

[3] A. K. Aziz and P. Monk. Continuous finite elements in space and time for the heat equation. *Math. Comp.*, 52(186):255–274, 1989.

[4] E. Burman and M. A. Fernández. Finite element methods with symmetric stabilization for the transient convection-diffusion-reaction equation. *Comput. Methods Appl. Mech. Engrg.*, 198(33-36):2508–2519, 2009.

[5] E. Burman and P. Hansbo. The edge stabilization method for finite elements in CFD. In *Numerical mathematics and advanced applications*, pages 196–203. Springer, Berlin, 2004.

[6] P. G. Ciarlet. *The finite element method for elliptic problems*. North-Holland Publishing Co., Amsterdam, 1978. Studies in Mathematics and its Applications, Vol. 4.

[7] R. Codina. Comparison of some finite element methods for solving the diffusion-convection-reaction equation. *Comput. Methods Appl. Mech. Engrg.*, 156(1-4):185–210, 1998.

[8] R. Codina. Stabilization of incompressibility and convection through orthogonal sub-scales in finite element methods. *Comput. Methods Appl. Mech. Engrg.*, 190(13-14):1579–1599, 2000.

[9] R. Codina and J. Blasco. Analysis of a stabilized finite element approximation of the transient convection-diffusion-reaction equation using orthogonal subscales. *Comput. Vis. Sci.*, 4(3):167–174, 2002.

[10] Miloslav Feistauer, Jaroslav Hájek, and Karel Svadlenka. Space-time discontinuous Galerkin method for solving nonstationary convection-diffusion-reaction problems. *Appl. Math.*, 52(3):197–233, 2007.

[11] E. Hairer and G. Wanner. *Solving ordinary differential equations. II*, volume 14 of *Springer Series in Computational Mathematics*. Springer-Verlag, Berlin, second edition, 1996. Stiff and differential-algebraic problems.

[12] L. He and L. Tobiska. The two-level local projection stabilization as an enriched one-level approach. *Adv. Comput. Math.*, 2011. DOI 10.1007/s10444-011-9188-1.

[13] T. J. R. Hughes and A. N. Brooks. A multidimensional upwind scheme with no crosswind diffusion. In *Finite element methods for convection dominated flows (Papers, Winter Ann. Meeting Amer. Soc. Mech. Engrs., New York, 1979)*, volume 34 of *AMD*, pages 19–35. Amer. Soc. Mech. Engrs. (ASME), New York, 1979.

[14] S. Hussain, F. Schieweck, and S. Turek. Higher order Galerkin time discretizations and fast multigrid solvers for the heat equation. *J. Numer. Math*, 19(1):41–61, 2011.

[15] V. John and G. Matthies. MooNMD—a program package based on mapped finite element methods. *Comput. Vis. Sci.*, 6(2-3):163–169, 2004.

[16] V. John and J. Novo. Error analysis of the SUPG finite element discretization of evolutionary convection-diffusion-reaction equations. *SIAM J. Numer. Anal.*, 49(3):1149–1176, 2011.

[17] V. John and E. Schmeyer. Finite element methods for time-dependent convection-diffusion-reaction equations with small diffusion. *Comput. Methods Appl. Mech. Engrg.*, 198(3-4):475–494, 2008.

[18] P. Knobloch. On the application of local projection methods to convection-diffusion-reaction problems. In *BAIL 2008—boundary and interior layers*, volume 69 of *Lect. Notes Comput. Sci. Eng.*, pages 183–194. Springer, Berlin, 2009.

[19] P. Knobloch. A generalization of the local projection stabilization for convection-diffusion-reaction equations. *SIAM J. Numer. Anal.*, 48(2):659–680, 2010.

[20] G. Lube and D. Weiss. Stabilized finite element methods for singularly perturbed parabolic problems. *Appl. Numer. Math.*, 17(4):431–459, 1995.

[21] G. Matthies and F. Schieweck. Higher order variational time discretizations for nonlinear systems of ordinary differential equations. Preprint 23/2011, Fakultät für Mathematik, Otto-von-Guericke-Universität Magdeburg, 2011.

[22] G. Matthies, P. Skrzypacz, and L. Tobiska. A unified convergence analysis for local projection stabilisations applied to the Oseen problem. *M2AN Math. Model. Numer. Anal.*, 41(4):713–742, 2007.

[23] H. G. Roos, M. Stynes, and L. Tobiska. *Robust numerical methods for singularly perturbed differential equations*, volume 24 of *Springer Series in Computational Mathematics*. Springer-Verlag, Berlin, second edition, 2008. Convection-diffusion-reaction and flow problems.

[24] F. Schieweck. *A*-stable discontinuous Galerkin-Petrov time discretization of higher order. *J. Numer. Math.*, 18(1):25–57, 2010.

[25] V. Thomée. *Galerkin finite element methods for parabolic problems*, volume 25 of *Springer Series in Computational Mathematics*. Springer-Verlag, Berlin, second edition, 2006.